J Therm Anal Calorim (2014) 116:887–894
DOI 10.1007/s10973-013-3595-0

Evolved gas analysis of coal-derived pyrite/marcasite

Hongfei Cheng · Qinfu Liu · Shuai Zhang · Shaoqing Wang · Ray L. Frost

Received: 1 September 2013 / Accepted: 9 December 2013 / Published online: 7 January 2014

Abstract The products evolved during the thermal decomposition of the coal-derived pyrite/marcasite were studied using simultaneous thermogravimetry coupled with Fourier-transform infrared spectroscopy and mass spectrometry (TG-FTIR–MS) technique. The main gases and volatile products released during the thermal decomposition of the coal-derived pyrite/marcasite are water (H_2O), carbon dioxide (CO_2), and sulfur dioxide (SO_2). The results showed that the evolved products obtained were mainly divided into two processes: (1) the main evolved product H_2O is mainly released at below 300 °C; (2) under the temperature of 450–650 °C, the main evolved products are SO_2 and small amount of CO_2. It is worth mentioning that SO_3 was not observed as a product as no peak was observed in the $m/z = 80$ curve. The chemical substance SO_2 is present as the main gaseous product in the thermal decomposition for the sample. The coal-derived pyrite/marcasite is different from mineral pyrite in thermal decomposition temperature. The mass spectrometric analysis results are in good agreement with the infrared spectroscopic analysis of the evolved gases. These results give the evidence on the thermal decomposition products and make all explanations have the sufficient evidence. Therefore, TG–MS–IR is a powerful tool for the investigation of gas evolution from the thermal decomposition of materials.

Keywords Pyrite · Marcasite · Thermal decomposition · Evolved gas · Sulfur dioxide

H. Cheng · Q. Liu (✉) · S. Zhang · S. Wang
School of Geoscience and Surveying Engineering, China University of Mining & Technology, Beijing 100083, People's Republic of China
e-mail: lqf@cumtb.edu.cn

H. Cheng
State Key Laboratory of Coal Resources and Safe Mining, China University of Mining & Technology, Beijing 100083, People's Republic of China

H. Cheng · R. L. Frost (✉)
School of Chemistry, Physics and Mechanical Engineering, Science and Engineering Faculty, Queensland University of Technology, 2 George Street, GPO Box 2434, Brisbane, QLD 4001, Australia
e-mail: r.frost@qut.edu.au

Introduction

Pyrite, with chemical formula FeS_2, is a quite frequently occurred mineral of sulfur and is found in a wide range of geological sites [1]. In nature, pyrite existed in the sulfur minerals and coal in the fine dispersed case as well as in free forms [2–4]. Pyritic and organic sulfur are the two major forms of sulfur in coal [5–9]. The wide occurrence of pyrite in different minerals and coals makes it one of the main sources of SO_2 emission from various industrial activities, such as the metallurgical industry, power production, and cement production. It was found that SO_2 is formed when pyrite is oxidized in industrial processes [10]. In countries such as China, pyrite is very abundant and dominant sulfide compound in coal. Although it is only composed of a relatively small portion of coal, it almost influences and decides the operational, environmental, and economic performance of handling and utilizing processes of coal [11, 12]. It might be one of the most striking examples of how the reactivity of pyrite can affect an environment associated with anthropogenic activities. The oxidative decomposition of pyrite in coal mining sites leads to the devastating environmental problem known as acid mine drainage [13]. This is because pyrite releases a major source of SO_2 (acid rain precursor) in

the combustion process and many evidences also suggest that it may possibly possess a catalytic role in coal liquefaction and gasification processes. Given the environmental concerns pyrite oxidation presents, there has been an intense scientific effort to understand the oxidation process and to develop methods to protect the pyrite surface from the deleterious effects of oxidation [14].

Several researchers have studied the thermal decomposition of pyrite. Eneroth and Koch [15] studied the thermal oxidation of pyrite and its polymorph, marcasite, by heating pyrite between 200 and 650 °C for 1 h in the presence of oxygen and reported hematite as the main product. Sit et al. [16] reported that the adsorption and reactions of water and O_2 with the FeS_2 (100) surface provide detailed mechanistic insight into pyrite oxidation and the complex electron flow accompanying this process. Oxidation of the pyrite surface occurs through successive reactions of the surface with adsorbed O_2 and water molecules. The gaseous degradation products seem also to be known for a long time from work of Hansen [17], who mentioned that measurable SO_2 formation is mainly caused by the oxidation of pyrite. However, an evolved gas analysis (EGA) study [18] only uses mass spectroscopic data to illustrate the oxidation products by identifying their presence from the characteristic thermal decomposition process, and the infrared spectroscopic analysis of evolved gaseous mixtures from pyrite was not mentioned in this study. A more recent similar study [12] carried out under inert atmosphere still contains some uncertainties in identification of the gaseous species evolved by the temperature-programed decomposition-mass spectrometer analysis.

In order to elucidate the basic reactions processes of thermal decomposition of pyrite in oxidative atmosphere, here we present our study on identification and tracking of evolving gaseous species from the coal-derived pyrite/marcasite pyrolysis using simultaneous thermogravimetry coupled with Fourier-transform infrared spectroscopy and mass spectrometry (TG-FTIR–MS). TG-FTIR–MS, a powerful method, has been used in previous studies to measure evolved gases during the thermal treatment of various substances [6, 19–22]. The components of released gaseous mixtures have been monitored and identified mostly on the basis of their FTIR and MS. Evolution curves obtained in flowing air by TG–MS–FTIR methods are compared in details [23–25]. This method offers the potential for the non-destructive, simultaneous, real-time measurement of multiple gas phase compounds in complex mixture.

Experimental methods

Materials

The coal-derived pyrite/marcasite sample used in the present investigation was extracted from the Qinshui coalfield, Shanxi province of China. The initial sample of the coal-derived pyrite/marcasite with particle size 0.1–0.2 mm was first subjected to gravity separation to remove the inclusions of coal using a laboratory mechanical pan (Micropaner). Then, the obtained concentrate was cleaned by means of magnetic separation. The mineral composition of the final product was estimated by X-ray diffraction (XRD). The XRD pattern for the coal-derived pyrite/marcasite is presented in Fig. 1.

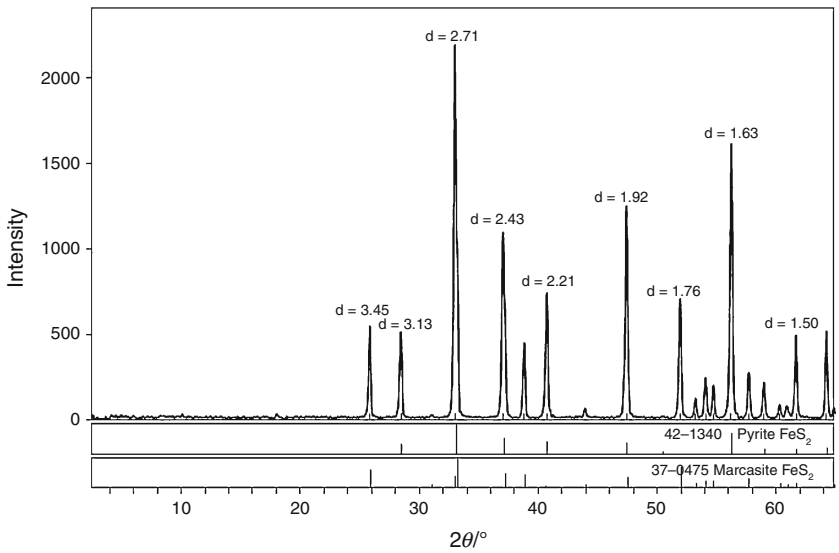

Fig. 1 XRD pattern for the coal-derived pyrite/marcasite

Characterization

X-ray diffraction (XRD)

The XRD pattern of the prepared sample was performed using a Rigaku D/max 2500PC X-ray diffractometer with Cu ($\lambda = 1.54178$ Å) irradiation at the scanning rate of 2° min^{-1} in the 2θ range of 2.6°–70°, operating at 40 kV and 150 mA.

In situ TG–MS–FTIR

The in situ TG-FTIR–MS analysis was performed using simultaneous thermogravimetry (Netzsch Sta 449 C) coupled with FTIR (Bruker Tensor 27) and mass spectrometry (ThermoStar, Pfeiffer Vacuum). About 10 mg of the sample was heated under air, a heating rate of 5 °C min^{-1} from 30 to 800 °C. The gas ionization was performed at 100 eV. The *m/z* was carried out from 1 to 100 atomic mass units (amu) to determine which *m/z* has to be followed during the TG experiments. The intensities of 11 selected ions (*m/z* = 15, 16, 17, 18, 32, 33, 34, 44, 48, 64, and 80) were monitored with the thermogravimetric parameters. However, the ion curves close to the noise level were omitted. Finally, only the intensities of nine selected ions (*m/z* = 16, 17, 18, 32, 34, 44, 48, 64, and 80) were discussed in mass spectrometric analysis. The bottom of the thermoanalyzer was heated to about 200 °C to eliminate cold points in the connecting line. The FTIR spectra were collected at a resolution of 4 cm^{-1}, and 200 scans were co-added per spectrum. The literature on the thermal decomposition of pyrite shows that the most important gaseous products evolved during devolatilization are SO_2 and SO_3. Therefore, although some ionic species, in this study, were produced during the pyrolysis, the following gaseous species were specially studied: CO_2, H_2O, SO_2, and SO_3.

Results and discussion

XRD results

The XRD pattern of the sample together with standard XRD patterns is shown in Fig. 1, which indicates that the sample contains mainly pyrite and marcasite. According to the quantitative XRD analysis, the mineral composition of the sample is shown in Table 1. Compared with the standard joint committee on powder diffraction standards (JCPDS) cards, the XRD pattern for the raw pyrite showed peak intensity at $2\theta = 28.51$, 33.08, 37.11, 40.78, 47.41, 50.49, 56.28 which suggested a very high degree of purity according to JCPDS file [12]. The crystallographic structure of pyrite as taken by the name-giving chemical compound of composition FeS_2 was among the earliest structures solved by XRD procedures. It was reported that the Fe ions build up a face-centered cubic lattice, into which the sulfur ions are embedded. The space lattice resembles that of sodium chloride, with Fe^{2+} replacing the sodium and S_2^{2-} replacing the chloride.

Table 1 The minerals composition of the coal-derived pyrite/marcasite used in this experiment

Mineral	Pyrite	Marcasite
Content of mineral/mass%	46.9	53.1

Pyrite has a cubic structure with lattice constant $a = 5.419$ Å, which is consistent with the previous literature [26]. Its space group is Pa3 with crystal cell molecules $Z = 4$. The crystalline size of the sample is about 20 nm, which is calculated from the XRD peaks using the Scherrer's formula. Although the structure of pyrite cannot be classified as essentially close packed, it is still a very dense material [27]. The four molecules in the unit cube are in special positions T_h^6 (Pa3). However, marcasite crystallizes in the orthorhombic system with a distinctive structure, which, like pyrite, gives it a self-identified position in the structure typology. Most of the data on marcasite and its isomorphs indicate a dimolecular unit, but faint reflections have suggested a tetramolecular cell. The structure is less dense than pyrite.

Thermal analysis

A typical record of the thermogravimetry and derivative thermogravimetric (TG–DTG) analysis curves of the coal-derived pyrite/marcasite is shown in Fig. 2. Six mass loss steps are observed (a) from 85 to 140 °C, (b) at 148 °C, (c) between 210 and 300 °C with the maximum rate at 251 °C, (d) three consecutive mass losses between 450 and 650 °C corresponded to mass losses of 12.34 % (450–520 °C), 8.07 % (520–575 °C), and 4.68 % (575–650 °C). The main reaction, as shown by both the TG and DTG curves, became apparent between 450 and 650 °C. According to the previous reports [17, 18, 28, 29], the thermal decomposition of pyrite mainly occurs at 450–480 °C, 530–570 °C, and 630–690 °C. The first mass loss of 4.76 % is attributed to loss of the adsorbed water. The second mass loss of 2.36 % is assigned to the loss of interparticle water for the sample. The third mass loss of 4.6 % between 200 and 300 °C with a maximum at 251 °C is due to the evolution of sulfur on the pyrite surface and loss of the rest part of interparticle water. Yan et al. [12] reported that the existence of elemental sulfur at pyrite surface has also been confirmed by other authors using Raman spectroscopy and X-ray photoelectron spectroscopy analysis. Three higher temperature decomposition steps are observed at

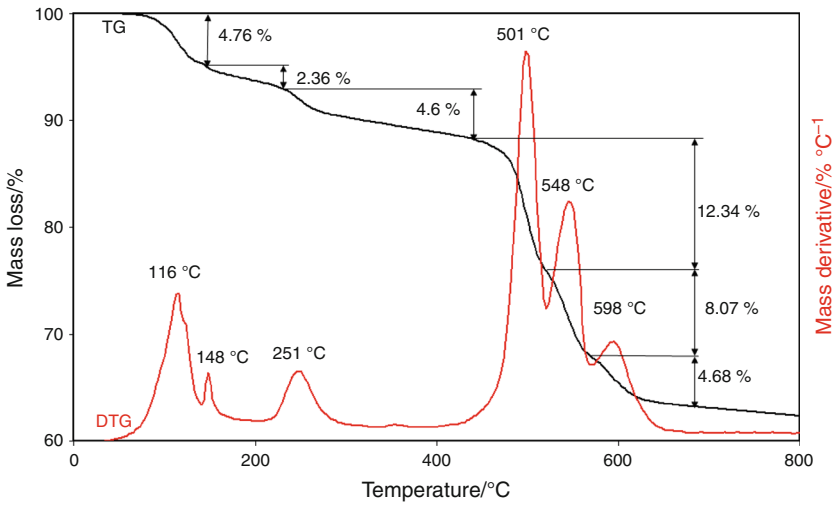

Fig. 2 TG–DTG curves of the coal-derived pyrite/marcasite

501, 548, and 598 °C with mass losses of 12.34, 8.07, and 4.68 % making a total mass loss at these temperatures of 25.09 %. In these three temperature steps, SO_2 is evolved which was confirmed by mass spectrometry. Therefore, the following decomposition is proposed [30].

$$FeS_2 + O_2 \rightarrow FeS + SO_2 \quad (1)$$

$$FeS_2 \rightarrow FeS + S \quad (2)$$

$$S + O_2 \rightarrow SO_2 \quad (3)$$

$$2FeS + \frac{7}{2}O_2 \rightarrow Fe_2O_3 + 2SO_2 \quad (4)$$

As a starting point for considering the mechanism of the reaction given by reaction (2), it was accepted that the thermal decomposition process of this reaction could be either a chemical reaction on the FeS_2/FeS interface, or the diffusion of sulfur vapor through the layer of FeS (pyrrhotite) [31]. It is also reported by Zivkovic et al. [32] that sulfur vapor appears in the pyrrhotite produced at a lower temperature (440–500 °C). Compared with the decomposition of pure pyrite in nitrogen, the initial decomposition temperature of the coal-derived pyrite/marcasite is nearly lower by 100 °C [18, 28, 29]. It suggests that the indigenous hydrocarbon with hydrogen donor ability in coal can promote the reduction of pyrite/marcasite, though the overall deficit of hydrogen makes the thermal decomposition reaction of pyrite/marcasite to prevail in pyrolysis [11]. It was reported that the decomposition of pyrite to pyrrhotite follows the unreacted core model [10, 28]. Therefore, the reaction (2) should be considered in thermal decomposition process without oxygen for the inner portion of pyrite particles.

It was stated both by Paulik et al. [28, 33] and Shkodin et al. [29] that three endothermic effects are observed in the thermoanalytical curves of pyrite: at 450–480 °C, 530–570 °C, and 630–690 °C, successively. The first endothermic effect in the thermoanalytical curves of pyrite in an inert gas stream at atmospheric pressure appears to be connected with the elimination of gaseous liquid inclusions. The second endothermic effect at 530–570 °C is interpreted as the decomposition process of the iron oxide sulfate film on the surface of the mineral and subsequent dissociation of pyrite, involving the removal of disulfide sulfur on its surface and formation of pyrrhotite on the freshly formed surface. The third effect is related to the dissociation of pyrite in its total bulk, yielding pyrrhotite and subsequently also troilite. The transformations at 450–480 °C and 530–570 °C, however, are interpreted differently by different researchers. Some authors [3] assume that the effect at 530–570 °C has no connection with the dissociation of pyrite, while data of other authors [4] indicate that pyrite partially dissociates, yielding pyrrhotite. According to Berg and co-workers [2], the endothermic effect at 450–480 °C is caused by evolved impurities and gaseous or liquid inclusions, and also by defects in the crystal lattice. The thermal process at 530–570 °C is attributed by these authors to the evolution of oxidized "non-equivalent" sulfur located on the surface of the pyrite. Simultaneously, they observed an increase in magnetic susceptibility, due to the appearance of pyrrhotite.

Mass spectrometric analysis of the evolved gases

The evolved products during the thermal decomposition of the coal-derived pyrite/marcasite were determined by thermogravimetry coupled to a mass spectrometer and are shown in Fig. 3. The interpretation of the mass spectra occurs on the basis of degassing profiles from the molecule ions of water vapor (H_2O: $m/z = 18$), carbon dioxide (CO_2: $m/z = 44$), sulfur dioxide (SO_2: $m/z = 64$), as well as by fragment ions (OH^+: $m/z = 17$, O^+: $m/z = 16$, ^{32}S : $m/z = 32$; $^{34}S^+$: $m/z = 34$, SO^+: $m/z = 48$).

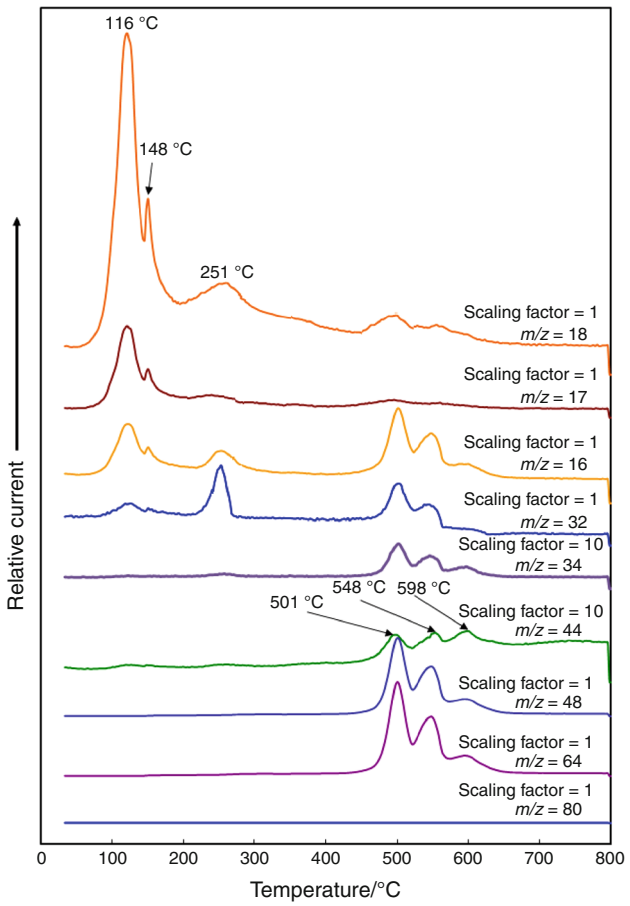

Fig. 3 Mass spectrometric analysis of the evolved gases for the coal-derived pyrite/marcasite

Combined with the TG–DTG analysis curves, six thermal decomposition steps are observed. The first step at 116 °C is due to loss of the adsorbed water molecules on the external surfaces of the mineral particles. The characterization of water release by means of MS is possible with the molecule ion H_2O^+ ($m/z = 18$) together with the fragment ion OH^+ ($m/z = 17$) and O^+ ($m/z = 16$). Peak at 148 °C for the sample is found in the ion current curve for H_2O^+ ($m/z = 18$); corresponding peaks are also found in the ion current curves for OH^+ ($m/z = 17$) and O^+ ($m/z = 16$). It can be safely concluded that water is given out at about 148 °C for the sample, which is consistent with the mass loss observed at about 148 °C from the TG curves. The third step at 251 °C is assigned to the evolution of sulfur on the pyrite surface and loss of the rest part of interparticle water. This result is in good agreement with the results of Thomas et al. [18]. The last three assignments are based on the MS data shown in Fig. 3. Peaks at 501, 548, and 598 °C for the sample are found in the ion current curve for SO_2^+ ($m/z = 64$); corresponding peaks are also found in the ion current curves for SO^+ ($m/z = 48$), ^{34}S ($m/z = 34$), and $^{32}S^+$ ($m/z = 32$). The evolution profiles of the ions at $m/z = 64$ (SO_2^+) and $m/z = 48$ (SO^+), the fragment ion, are used to identify the presence of SO_2. The $m/z = 64$ and 48 peaks observed to follow the TG–DTG peaks indicating the evolution of SO_2 during both the steps of the thermal decomposition. It is observed that the final product of the decomposition, as determined from XRD, was hematite (Fe_2O_3) which is in agreement with the previous literature [18]. It is also reported by Jorgensen and Moyle [34] that hematite (Fe_2O_3) is the solid end product of the reaction in this temperature range. They further concluded that small amounts of pyrrhotite formed as thin layers of intermediate reaction product but in amounts which are small in comparison with the amount of hematite. Thus, Eq. (4) is a reasonable candidate for this process. It is also indicated that the chemical substance SO_2 is present in the thermal decomposition for the sample, and this will be further proved by the following IR results.

The three broad peaks at 501, 548, and 598 °C are found in the ion current curve for CO_2 ($m/z = 44$). This illustrates that a small proportion of CO_2 is given out in this temperature range. This may be due to the pyrolysis of the residual coal. It is also observed that the relative intensity of CO_2 increases as temperature goes up. The MS data, using $m/z = 80$ curve, for this decomposition process indicated that no SO_3 was produced.

It is interesting to note that the three temperature peaks occurred one after another and the corresponding temperature range overlaps each other during thermal decomposition process. This phenomenon suggests that coal-derived pyrite/marcasite undergoes the decomposition till 650 °C and different transition states appeared one after another during the decomposition. Clearly, there are at least three transition state structures with different Fe/S values during thermal decomposition, which corresponds with the temperature peaks on MS profile. It should be noted that SO_3 was not observed as a product as no peak was observed in the $m/z = 80$ curve. It has been reported that mineral pyrite is slightly different from coal pyrite in reactivity due to their surface structure and morphology [3, 35]. The investigation by Sundaram [35] revealed that oxidation rate of coal pyrite was twice as high as that of mineral pyrite at 5 % oxygen, and four times as high as that of mineral pyrite at 10 % oxygen. Therefore, compared with the decomposition of pure pyrite, the initial decomposition temperature of the coal-derived pyrite/marcasite is nearly lower by 100 °C [18, 28, 29, 36, 37].

According to experimental results of the mass spectrometric analysis, the gaseous species produced by the thermal decomposition using the mass spectra made evident the following:

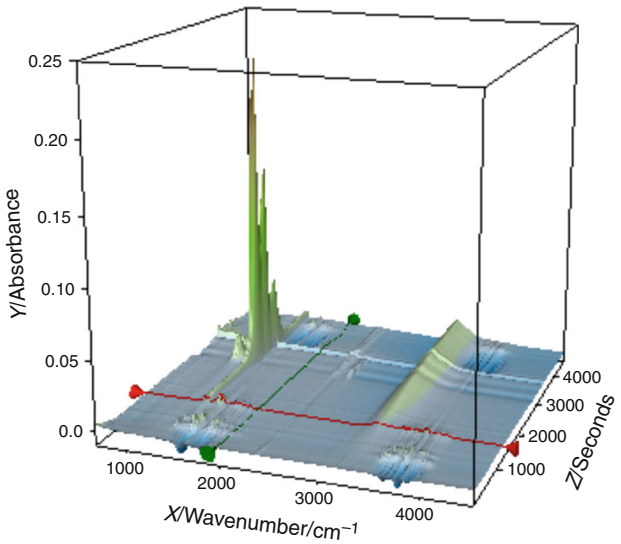

Fig. 4 3D FTIR spectra of the evolved gases for the coal-derived pyrite/marcasite

(a) The evolved products at 116, 148 °C: water;
(b) The evolved products at 251 °C: sulfur vapor and water;
(c) The evolved products at 501, 548, and 598 °C: sulfur dioxide, carbon dioxide, and water.

Based on these results, it can be concluded that the thermal decomposition of pyrite to pyrrhotite follows the unreacted core model between 450 and 520 °C. Pyrite can be oxidized directly or oxidized after it is firstly decomposed into pyrrhotite and sulfur. Hematite (Fe_2O_3) is the solid end product of the reaction in the temperature range of 550–650 °C, and SO_3 was not observed as a product for the thermal decomposition of the coal-derived pyrite/marcasite. It is indicated that the chemical substance SO_2 is present as the main gaseous product in the thermal decomposition for the sample. The coal-derived pyrite/marcasite is different from mineral pyrite in reactivity due to its surface structure and morphology.

Infrared spectroscopy analysis of the evolved gases

Figure 4 shows 3D FTIR spectra for the gases produced from the thermal decomposition of the coal-derived pyrite/marcasite. By comparing the spectra over the range 30–800 °C, it is important to note that the spectra not only provide the information about the species of the released gas, but also display the relative intensities of the evolved gas. It can be observed from the spectra that the pyrolysis products for the sample mainly vary in amounts but not in species. Combined with the mass spectroscopic analysis, main products are identified as follows: water (H_2O), carbon dioxide (CO_2), and sulfur dioxide (SO_2). The emission of sulfur dioxide (SO_2) is confirmed by the appearance of absorption bands in the range 1,300–1,450 cm^{-1} and 1,150 cm^{-1}. The characteristic bands of CO_2 at 2,217–2,391 cm^{-1} indicate its formation. The emission of water follows three steps. At low temperature, the absorbed water is released out by evaporation. Moreover, when the temperature reaches 150 °C, water was generated by the loss of interparticle water for the sample. In addition, an amount of water released out according to the characteristic band at 3,500–3,850 cm^{-1}.

FT-IR spectra of thermal decomposition products of the coal-derived pyrite/marcasite at different temperatures are shown in Fig. 5. As the temperature of the system is raised, the emission of water (H_2O) mainly occurred between 100 and 200 °C, and this temperature range of mass loss is attributed to the loss of absorbed water for the sample. At the same time, the sulfur dioxide (SO_2) is still detected by the in situ FTIR spectroscopic EGA. The evolved process within 450–650 °C can be divided into three parts: the first evolved process for the SO_2 with the maximum rate at 500 °C, and this temperature range of losing these two types of products is assigned to the oxidation of the sample particle surface and the decomposition of the interior for the pyrite particle without oxygen; the second evolved process for the SO_2 with a maximum at 550 °C is due to the evolution of oxidized sulfur stemmed from the last step of the decomposition of the pyrite particle without oxygen, Eq. (3); the third evolved process for the SO_2 with a maximum at 600 °C is attributed to the oxidation of the pyrrhotite, Eq. (4). According to the report by Hong and Fegley [36], no hematite (Fe_2O_3) but only pyrrhotite was observed within the temperature range of 400–520 °C. Paulik et al. [28] found that Eq. (2) should be considered in thermal decomposition process without oxygen for the inner portion of pyrite particles. Therefore, it is concluded that the mass loss at 450–521 °C is caused by the oxidation of the sample particle surface and the decomposition of the interior for the pyrite particle without oxygen, in accordance with Eqs. (1) and (2). A conclusion can be drawn that the mass loss in this stage is mainly caused by the release of SO_2, with the unique existence of characteristic bands at 1,300–1,450 and 1,150 cm^{-1}. It is also observed that a small amount of the CO_2 and the water are released in this temperature range. The absorption bands of volatile for the sample also appear to be at the same wavenumbers, while the diversities of the absorbance only exist in 1,300–1,450 cm^{-1} region. The release of water and CO_2 (bands at 3,500–3,850 and 2,217–2,391 cm^{-1} region) is less violent, while the relative intensity of SO_2 firstly increases and then decreases. It is reported that pyrrhotite is an intermediate phase produced during heating of pyrite [38]. The researchers further proposed that hematite is the major reaction product during heating pyrite in a restrictive

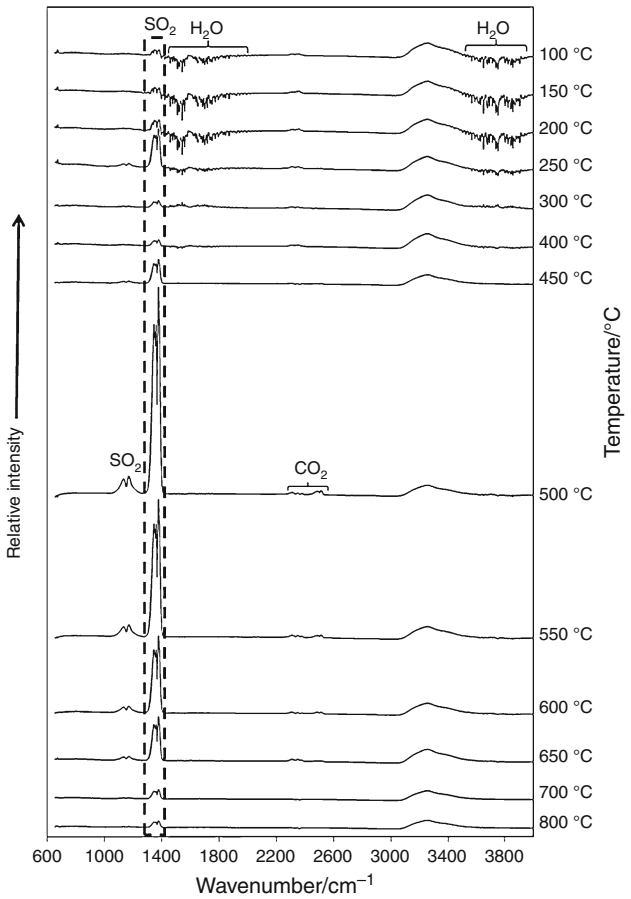

Fig. 5 Infrared spectroscopy analysis of the evolved gases for the coal-derived pyrite/marcasite

oxidative environment. Thus, Eq. (4) is a reasonable candidate for the last decomposition process.

Based on the results of this study and through reviewing and summarizing various study results, it can be concluded that the coal-derived pyrite/marcasite first decomposed to form pyrrhotite. The formed pyrrhotite was then oxidized to form oxides. The analysis showed the existence of pyrite, marcasite, pyrrhotite, and hematite at the later stage of the roasting process. This is an indication of the occurrence of simultaneous thermal decomposition of the pyrite and the oxidation of the formed pyrrhotite.

Conclusions

The products evolved during the thermal decomposition of the coal-derived pyrite/marcasite were studied using TG-FTIR–MS technique. The main mass losses for the thermal decomposition of the coal-derived pyrite/marcasite were observed at 116, 148, 251, 501, 548, and 598 °C which were attributed to (a) loss of the adsorbed water, (b) the loss of interparticle water for the sample, (c) the evolution of sulfur on the pyrite surface and loss of the rest part of interparticle water, (d) the oxidation of the sample particle surface and the decomposition of the interior for the pyrite particle without oxygen, (e) the evolution of oxidized sulfur stemmed from the last step of the decomposition of the pyrite particle without oxygen, and (f) the oxidation of the pyrrhotite. These thermal decomposition processes and products were proved by the mass spectrometric analysis and infrared spectroscopic analysis of the evolved gases.

The main gases and volatile products released during the thermal decomposition of the coal-derived pyrite/marcasite are water vapor (H_2O), carbon dioxide (CO_2), and sulfur dioxide (SO_2). The evolved products obtained were mainly divided into two processes: (1) the main evolved product H_2O is mainly released at below 300 °C; (2) under the temperature of 450–650 °C, the main evolved products are SO_2 and small amount of CO_2. It should be noted that SO_3 was not observed as a product as no peak was observed in the $m/z = 80$ curve. The oxidation of the coal-derived pyrite/marcasite starts at about 450 °C, and pyrrhotite and hematite are formed as primary products. The chemical substance SO_2 is present as the main gaseous product in the thermal decomposition process for the sample. The coal-derived pyrite/marcasite is vastly different from mineral pyrite in thermal decomposition temperature due to its surface structure and morphology. The mass spectrometric analysis results are in good agreement with the infrared spectroscopic analysis of the evolved gases. Thermal analysis and mass spectrometric analysis clearly show at which temperature the mass loss was observed. However, infrared spectroscopic analysis will give the evidence on the thermal decomposition products. These results make all explanations have the sufficient evidence. Therefore, thermal analysis coupled with spectroscopic gas analysis is demonstrated to be a powerful tool for the investigation of gas evolution from the thermal decomposition of materials. Using different gas analyzing methods like MS and FTIR increases the unambiguous interpretation of the results.

Acknowledgements The authors gratefully acknowledge the financial support provided by the National Natural Science Foundation of China (No. 51034006), the Beijing Joint-Construction Project (20121141301), and the Open Research Project of State Key Laboratory for Coal Resources and Safe Mining, China University of Mining &Technology (SKLCRSM11KFB06).

References

1. Hu H, Chen Q, Yin Z, Zhang P. Thermal behaviors of mechanically activated pyrites by thermogravimetry (TG). Thermochim Acta. 2003;398:233–40.
2. Boyabat N, Özer AK, Bayrakçeken S, Gülaboglu MS. Thermal decomposition of pyrite in the nitrogen atmosphere. Fuel Process Technol. 2004;85:179–88.

3. Bylina IV, Mojumdar SC, Papangelakis VG. Effect of storage time on the pressure oxidation enthalpy of pyrite. J Therm Anal Calorim. 2012;108:829–35.
4. Iliyas A, Hawboldt K, Khan F. Kinetics and safety analysis of sulfide mineral self-heating. J Therm Anal Calorim. 2011;106:53–61.
5. Gryglewicz G, Wilk P, Yperman J, Franco DV, Maes II, Mullens J, Van Poucke LC. Interaction of the organic matrix with pyrite during pyrolysis of a high-sulfur bituminous coal. Fuel. 1996;75:1499–504.
6. Kaljuvee T, Keelman M, Trikkel A, Petkova V. TG-FTIR/MS analysis of thermal and kinetic characteristics of some coal samples. J Therm Anal Calorim. 2013;113:1063–71.
7. Babiński P, Łabojko G, Kotyczka-Morańska M, Plis A. Kinetics of coal and char oxycombustion studied by TG-FTIR. J Therm Anal Calorim. 2013;113:371–8.
8. Cui X, Zhang X, Yang M, Feng Y, Gao H, Luo W. Study on the structure and reactivity of corex coal. J Therm Anal Calorim. 2013;113:693–701.
9. Liu Z, Zhang Y, Zhong L, Orndroff W, Zhao H, Cao Y, Zhang K, Pan W-P. Synergistic effects of mineral matter on the combustion of coal blended with biomass. J Therm Anal Calorim. 2013;113:489–96.
10. Hu G, Dam-Johansen K, Wedel S, Hansen JP. Decomposition and oxidation of pyrite. Prog Energ Combust. 2006;32:295–314.
11. Chen H, Li B, Zhang B. Decomposition of pyrite and the interaction of pyrite with coal organic matrix in pyrolysis and hydropyrolysis. Fuel. 2000;79:1627–31.
12. Yan J, Xu L, Yang J. A study on the thermal decomposition of coal-derived pyrite. J Anal Appl Pyrol. 2008;82:229–34.
13. Murphy R, Strongin DR. Surface reactivity of pyrite and related sulfides. Surf Sci Rep. 2009;64:1–45.
14. Zhang X, Borda MJ, Schoonen MAA, Strongin DR. Adsorption of phospholipids on pyrite and their effect on surface oxidation. Langmuir. 2003;19:8787–92.
15. Eneroth E, Koch CB. Crystallite size of haematite from thermal oxidation of pyrite and marcasite—effects of grain size and iron disulphide polymorph. Miner Eng. 2003;16:1257–67.
16. Sit PHL, Cohen MH, Selloni A. Interaction of oxygen and water with the (100) surface of pyrite: mechanism of sulfur oxidation. J Physic Chem Lett. 2012;3:2409–14.
17. Hansen JP, Jensen LS, Wedel S, Dam-Johansen K. Decomposition and oxidation of pyrite in a fixed-bed reactor. Ind Eng Chem Res. 2003;42:4290–5.
18. Thomas P, Hirschausen D, White R, Guerbois J, Ray A. Characterisation of the oxidation products of pyrite by thermogravimetric and evolved gas analysis. J Therm Anal Calorim. 2003;72:769–76.
19. Ahamad T, Alshehri SM. TG-FTIR–MS (evolved gas analysis) of bidi tobacco powder during combustion and pyrolysis. J Hazard Mater. 2012;199–200:200–8.
20. Madarász J, Brăileanu A, Crişan M, Pokol G. Comprehensive evolved gas analysis (EGA) of amorphous precursors for s-doped Titania by in situ TG-FTIR and TG/DTA-MS in air: part 2. Precursor from thiourea and Titanium(iv)-*n*-butoxide. J Anal Appl Pyrol. 2009;85:549–56.
21. Madarász J, Varga PP, Pokol G. Evolved gas analyses (TG/DTA–MS and TG-FTIR) on dehydration and pyrolysis of magnesium nitrate hexahydrate in air and nitrogen. J Anal Appl Pyrol. 2007;79:475–8.
22. Madarász J, Pokol G. Comparative evolved gas analyses on thermal degradation of thiourea by coupled TG-FTIR and TG/DTA–MS instruments. J Therm Anal Calorim. 2007;88:329–36.
23. Fischer M, Wohlfahrt S, Saraji-Bozorgzad M, Matuschek G, Post E, Denner T, Streibel T, Zimmermann R. Thermal analysis/evolved gas analysis using single photon ionization. J Therm Anal Calorim. 2013;113:1667–73.
24. Arockiasamy A, Toghiani H, Oglesby D, Horstemeyer MF, Bouvard JL, King R. TG–DSC–FTIR–MS study of gaseous compounds evolved during thermal decomposition of styrene-butadiene rubber. J Therm Anal Calorim. 2013;111:535–42.
25. Bednarek P, Szafran M. Thermal decomposition of monosaccharides derivatives applied in ceramic gelcasting process investigated by the coupled DTA/TG/MS analysis. J Therm Anal Calorim. 2012;109:773–82.
26. Qian XF, Zhang XM, Wang C, Tang KB, Xie Y, Qian YT. Solvent-thermal preparation of nanocrystalline pyrite cobalt disulfide. J Alloy Compd. 1998;278:110–2.
27. Lowson RT. Aqueous oxidation of pyrite by molecular oxygen. Chem Rev. 1993;82:461–97.
28. Paulik F, Paulik J, Arnold M. Kinetics and mechanism of the decomposition of pyrite under conventional and quasi-isothermal—quasi-isobaric thermoanalytical conditions. J Therm Anal Calorim. 1982;25:313–25.
29. Shkodin VG, Abishev DN, Kobzhasov AK, Malyshev VP, Mangutova RF. The question of thermal decomposition of pyrite. J Therm Anal Calorim. 1978;13:49–53.
30. Cheng H, Liu Q, Huang M, Zhang S, Frost RL. Application of TG-FTIR to study SO_2 evolved during the thermal decomposition of coal-derived pyrite. Thermochim Acta. 2013;555:1–6.
31. Jovanović D. Kinetics of thermal decomposition of pyrite in an inert atmosphere. J Therm Anal Calorim. 1989;35:1483–92.
32. Zivkovic ZD, Mitevska N, Savovic V. Kinetics and mechanism of the chalcopyrite-pyrite concentrate oxidation process. Thermochim Acta. 1996;282–283:121–30.
33. Paulik J, Paulik F, Arnold M. Simultaneous TG, DTG, DTA and EGA technique for the determination of carbonate, sulphate, pyrite and organic material in minerals, soils and rocks. J Therm Anal Calorim. 1982;25:327–40.
34. Jorgensen FRA, Moyle FJ. Gas diffusion during the thermal analysis of pyrite. J Therm Anal Calorim. 1986;31:145–56.
35. Sundaram HP, Cho EH, Miller A. SO_2 removal by leaching coal pyrite. Energ Fuel. 2001;15:470–6.
36. Hong Y, Fegley B. The kinetics and mechanism of pyrite thermal decomposition. Ber Bunsenges Phys Chem. 1997;101:1870–81.
37. Cleyle PJ, Caley WF, Stewart L, Whiteway SG. Decomposition of pyrite and trapping of sulphur in a coal matrix during pyrolysis of coal. Fuel. 1984;63:1579–82.
38. Bhargava SK, Garg A, Subasinghe ND. In situ high-temperature phase transformation studies on pyrite. Fuel. 2009;88:988–93.